Antenna Selection Strategy for Transmit Beamforming-based Joint Radar-Communication System

Ammar Ahmed, Shuimei Zhang, Yimin D. Zhang

Department of Electrical and Computer Engineering, Temple University,
Philadelphia, PA 19122, USA

Abstract

Antenna array-based joint radar-communication (JRC) system employs the beamforming strategy to steer the transmit signals in different directions such that different beamforming weight vectors are exploited which perform the corresponding radar-communication objectives. Such functionality has been provisioned in the spectrally congested environments where both systems are destined to coexist. The transmit antenna selection has become an increasingly interesting topic as the antennas become significantly cheaper and smaller relative to the up-conversion chains. In this paper, we address the problem of antenna selection for the JRC system by employing a re-weighted l_1-norm minimization naturally yielding the low-complexity solution compared to the exhaustive l_0-norm-based optimization. We present the mathematical framework for the proposed approach in the context of the individual as well as grouped beamforming weight vectors and analyze the practical applicability of the proposed approach for both cases. We argue that the grouped approach for optimizing the JRC antenna selection is hardware-efficient compared to the antenna selection for individual beamforming weight vectors. Simulation results illustrate that the proposed technique significantly reduces the number of required antennas while simultaneously satisfying the radar and communication system objectives.

Keywords: Antenna selection, Beamforming, Convex optimization, Joint radar-communication, Sparse antenna array, Spectral congestion, Spectrum sharing.

I. Introduction

Spectrum sharing has gained significant attention of researchers due to the ongoing increase in the demand of spectral resources [2–6]. In this context, extensive efforts have been invested to discuss the co-existence of the multiple platforms within the same spectral bands [7–29]. Successful deployment of co-existing radar-communication systems within the same spectral and time resource can only be realized when both systems cooperate to mollify the interference between them. Such an objective can be significantly simplified if both systems are controlled by the same control entity that carries out both radar and communication tasks. Joint radar-communication (JRC) systems are the examples of such systems which exploit the same physical platform to satisfy the objectives of both subsystems [6, 10, 12, 13, 15, 17–22, 24, 29].

In a JRC system, the dual-purpose transmit waveforms serve both radar and communication objectives and are transmitted using the same physical platform. The radar and communication operations are respectively considered to be the primary and secondary tasks of the JRC system, i.e., the radar task is given the supreme precedence. Several configurations of JRC systems have been discussed in the literature. Single antenna transmitter-based JRC systems usually employ waveform diversity to transmit the communication information where the same waveforms serve the radar objectives [2, 3, 12, 22]. The notable sidelobe control-based JRC strategies developed so far include the sidelobe amplitude modulation (AM) method [10], multi-waveform amplitude shift keying (ASK) method [15, 18], phase shift keying (PSK) method [16], and sidelobe quadrature amplitude modulation (QAM) method [25]. In the sidelobe AM method [10], an antenna array is employed to transmit most of the power for the radar mission, whereas the communication operation is enabled in the radar sidelobe region by changing the sidelobe amplitude levels in the directions of the communication users. In such a technique, each sidelobe level is mapped to a unique communication symbol. Multi-waveform ASK-based method [15, 18]

2

exploits multiple orthogonal radar waveforms along with the sidelobe amplitude modulation which increases the communication data rate by employing waveform diversity. Matched filtering is used at the communication receivers which extracts the transmitted sidelobe amplitudes to decode the transmitted communication information. In PSK-based JRC schemes [16], the communication information is embedded in the radar waveforms by employing a dictionary of beamforming weight vectors having the same beampattern but different phase response towards the communication receivers. The sidelobe QAM modulation [25] enjoys further flexibility by changing both transmit amplitudes and phases towards the communication user directions, resulting in an enhanced communication data rate. On the other hand, the distributed JRC systems exploit waveform diversity and spatial diversity to carry out concurrent radar and communication operations [25].

In a JRC transmitter, a radio transmission chain, which consists of a digital-to-analog converter, a mixer, and a power amplifier, is often much more expensive than the transmit antennas. Therefore, to achieve a high system performance at a low cost, a recent trend is to place more antennas than the available number of expensive radio transmission chains. Ideally, it is desirable to automatically switch the available chains to the best subset of antennas which provides the optimized performance for the whole system. Therefore, optimal antenna selection has a crucial importance in the modern systems. Several research efforts have been made in this direction for different radar and communication applications. In [30], antenna selection has been discussed for a distributed multiple-input and multiple output (MIMO) radar to achieve the radar's objective in terms of desired mean-squared error. For the communication systems, [31–33] discuss the antenna selection strategies using convex optimization and sparsity-aware techniques. Distributed JRC systems also enjoy optimal transmit antenna selection such that the desired communication capacity and radar performance are achieved [25]. For antenna array-based JRC systems, an array partitioning-based approach is employed in [34] where the functional antennas are split into two subarrays respectively performing the
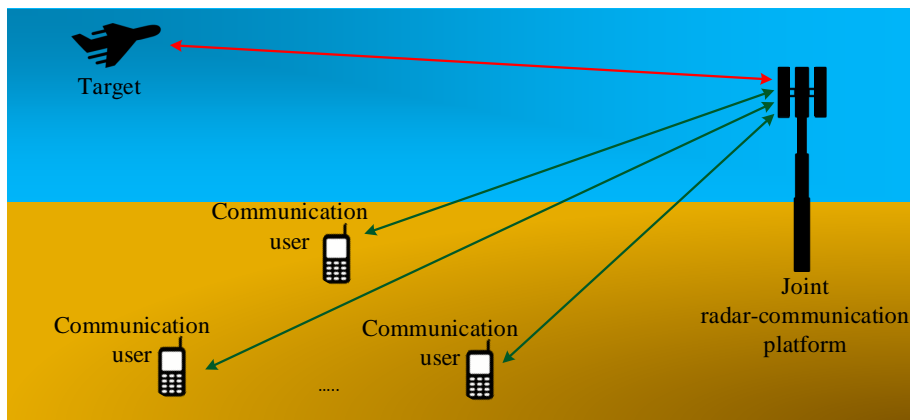
3

Figure 1: Basic principle of the joint radar-communication system.

radar and communications operations. Similarly, [35] addresses the optimal antenna selection at the receiver side of JRC systems to maximize the signal-to-interference-plus-noise ratio. Iterative optimization-based optimal antenna selection for array-based JRC schemes was discussed in [36, 37]. Note that the existing antenna array-based JRC antenna selection schemes employing the sidelobe modulation principle select different antennas for different beamforming weight vectors. Such a scenario results in frequent and unavoidable antenna switching during the JRC operation, complicating the hardware implementation and degrading the applicability in practice.

In this paper, our focus is on antenna array-based JRC system which exploits beamformers to perform radar operation whereas the communication operation is enabled in the radar sidelobe region by employing QAM-based sidelobe modulation. The waveforms responsible to perform the radar task are also utilized to satisfy the requirements of the communication system. An example of such a system is illustrated in Fig. 1. The radar objective in this JRC system is to maintain a specific beamforming gain in the sector of radar interest. The communication information is transmitted by varying the transmit amplitudes as well as the phases towards the communication user directions located in the sidelobe region of the radar. The objective of our optimization approach is to

4

select the minimum number of antennas which satisfy the required radar and communications operations. We present the convex optimization-based mathematical formulation which addresses this objective in two different ways. First, we present an optimal antenna selection strategy for individual beamforming weight vectors employing the QAM-based sidelobe modulation approach. As the selected antennas for different beamformers are generally different, the resulting solutions can result in frequent antenna switching. To tackle this problem, we also develop a group sparsity-based approach in which the same set of antennas is used for all beamformers without any antenna switching.

The rest of the paper is organized as follows. Section II presents the JRC system model. In Section III, we present the proposed optimal antenna selection strategy for the JRC system. Comparative analysis of the proposed approaches is provided in Section IV. Simulation results are presented in Section V, and Section VI concludes the paper.

Notations: Lower-case (upper-case) bold characters are used to denote vectors (matrices). $(\cdot)^*$, $(\cdot)^{\mathrm{T}}$ and $(\cdot)^{\mathrm{H}}$ represent the conjugate, transpose and the Hermitian transpose operators, respectively. $|\cdot|$, $\|\cdot\|_0$, $\|\cdot\|_1$, and $\|\cdot\|_2$ denote the absolute value, l_0-, l_1- and l_2-norms, respectively. Moreover, $\mathbf{1}_{K\times 1}$ denotes the K-length column vector of all ones, $\odot$ represents the Hadamard product, and C is the combination operator.

II. Signal Model of JRC system

We consider an antenna array-based JRC system consisting of M-element transmit linear array of an arbitrary configuration. The JRC system employs the antenna array beamformers to satisfy the transmit gain objective within the radar main beam. The same beamformers are responsible to transmit communication information within the sidelobe region such that the radar operation is not perturbed.

Consider the radar surveillance region, the sidelobe region, and the transition region from main beam to sidelobe denoted by Θ_{rad}, Θ_{sl}, and Θ_{trans}, respec-

tively. There are a total of C communication users located within the sidelobe region of the radar. The objective of JRC antenna array is to maintain the transmit gain G_{rad} in the main beam of the radar, whereas the sidelobe region of the radar should be lower than a threshold $\varepsilon_{\mathrm{sl}}$. The communication operation should be enabled by transmitting distinct phases and amplitudes towards the communication receivers. The beamforming weight vector $\mathbf{w}_n$ which satisfies these objectives can be extracted using the following optimization [6, 15, 20]:

$$
\begin{aligned}
\min_{\mathbf{w}_n} \max_{\theta_r} & \left| G_{\mathrm{rad}} e^{j\varphi(\theta_r)} - \mathbf{w}_n^{\mathrm{H}} \mathbf{a}(\theta_r) \right|, & \theta_r \in \Theta_{\mathrm{rad}}, \\
\text{subject to } & \left| \mathbf{w}_n^{\mathrm{H}} \mathbf{a}(\theta_\varepsilon) \right| \leq \varepsilon_{\mathrm{sl}}, & \theta_\varepsilon \in \Theta_{\mathrm{sl}}, \\
& \mathbf{w}_n^{\mathrm{H}} \mathbf{a}(\theta_c) = e^{j\phi_{n,c}} \Delta_{n,c}, & c = 1, \cdots, C.
\end{aligned}
\tag{1}
$$

where $\mathbf{w}_n$ achieves the sidelobe level $\Delta_{n,c}$ and the phase $e^{j\phi_{n,c}}$ towards the cth $(c = 1, \cdots, C)$ communication receiver located at angle θ_c such that $\theta_c \in \Theta_{\mathrm{sl}}$. The parameter $e^{j\varphi(\theta_r)}$ represents the phase profile of the radar in the main beam. We use the phase profile $e^{j\varphi(\theta_r)}$ as a free parameter in the above optimization in order to achieve better approximation of the desired beampattern [36]. Such phase response can be first extracted by designing a beamforming weight vector which only satisfies the radar objective within the main beam. Also, there are other phase adjustment techniques as in [36, 38]. The array response vector of the JRC transmit system at the angle θ is given by

$$
\mathbf{a}(\theta) = [e^{j2\pi d_1 \sin(\theta)/\lambda}, e^{j2\pi d_2 \sin(\theta)/\lambda}, \ldots, e^{j2\pi d_M \sin(\theta)/\lambda}]^{\mathrm{T}},
$$

where d_m is the location of mth $(m = 1, \cdots, M)$ antenna and λ is the transmit signal wavelength.

The optimization (1) can be exploited to extract a dictionary of N beamforming vectors where each vector transmits a specific phase and magnitude towards different communication receivers. Note that the optimization (1) enables multiple-access communication as the values of $\Delta_{n,c}$ and $e^{j\phi_{n,c}}$ can be different for each communication receiver for the same beamformer. If L and P respectively denote the desired possible number of amplitudes and phases at each communication receiver, we will require $N = (LP)^C$ unique beamforming

weight vectors. Note that if Θ_{rad} contains only one angle, the optimization (1) corresponds to the focused beampattern design. On the other hand, if Θ_{rad} contains multiple angles corresponding to a sector, the optimization (1) corresponds to the flat-top beampattern synthesis.

The JRC system exploits dual-purpose waveforms, i.e. the same waveforms which serve the radar purpose are also utilized to perform the communication operation. Consider that the JRC system exploits K possible orthogonal dual-purpose waveforms $\psi_1(t), \psi_2(t), \ldots, \psi_K(t)$ such that:

$$\frac{1}{T} \int_0^T \psi_{k_1}(t) \, \psi_{k_2}(t - \Delta T) \mathrm{d}t = \delta\left(k_1 - k_2 - \Delta T\right), \quad 1 \le k_1, k_2 \le K, \qquad (2)$$

where t denotes the fast time, T is the time duration of each radar pulse, k_1 and k_2 are the positive integers, $\delta(\cdot)$ is the Kronecker delta function, and $\psi_{k_2}(t - \Delta T)$ denotes the time delayed version of $\psi_{k_2}(t)$ such that $\Delta T < T$.

When the beamforming vector $\mathbf{w}_n$ is selected, the transmit signal from the JRC antenna array takes the following form:

$$\mathbf{x}(t) = \mathbf{w}_n \psi_k(t). \qquad (3)$$

The above beamforming vector satisfies the gain criteria of the main beam and projects the QAM symbols of amplitude $\Delta_{n,c}$ and phase $e^{j\phi_{n,c}}$ towards the communication directions. The JRC system can change the transmitted communication information by changing the beamforming vectors [20].

III. Transmit Antenna Selection Strategy for JRC System

We propose the antenna selection strategy for transmit beamforming-based JRC system as illustrated in Fig. 2. Our objective is two-fold: Design the beamforming weight vector for the JRC system which (a) use the least possible number of antennas, (b) exploit minimum transmit power. As both objectives can be conflicting, we give more precedence to the first objective. In this context, two cases are discussed. In the first case, transmit antennas are selected for each beamforming weight vector separately. This strategy might result in the
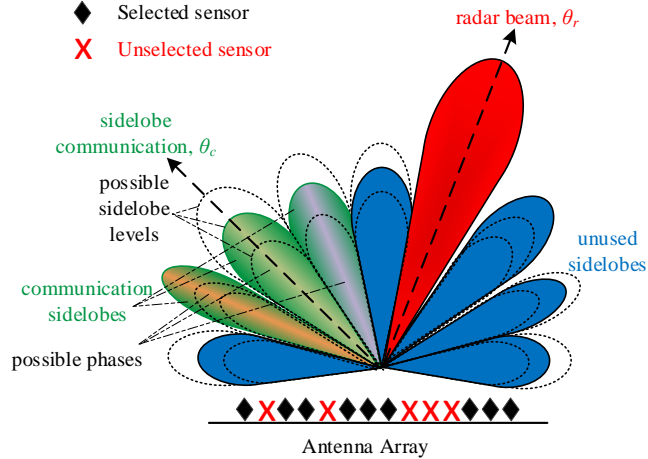
7

Figure 2: The proposed antenna selection strategy for joint radar-communication system.

activation of different antennas for different beamforming weight vectors. On the other hand, the second approach discusses the joint antenna selection strategy for multiple beamforming weight vectors which exploits the same antennas for all the beamforming weight vectors without any antenna switching.

A. Transmit Antenna Selection for Individual Beamformers

For a given JRC antenna array, beamforming weight vector which minimizes the total transmit power $\|\mathbf{w}_n\|_2^2$ can be expressed as follows:

$$
\begin{aligned}
\min_{\mathbf{w}_n} \quad & \|\mathbf{w}_n\|_2^2 \\
\text{subject to} \quad & |G_{\mathrm{rad}}e^{j\varphi(\theta_r)} - \mathbf{w}_n^{\mathrm{H}}\mathbf{a}(\theta_r)| \leq \gamma_{\mathrm{tol}}, \quad \theta_r \in \Theta_{\mathrm{rad}}, \\
& |\mathbf{w}_n^{\mathrm{H}}\mathbf{a}(\theta_\varepsilon)| \leq \varepsilon_{\mathrm{sl}}, \qquad\qquad\quad \theta_\varepsilon \in \Theta_{\mathrm{sl}}, \\
& \mathbf{w}_n^{\mathrm{H}}\mathbf{a}(\theta_c) = \Delta_{n,c}e^{j\phi_{n,c}}, \qquad\quad c = 1,\cdots,C,
\end{aligned}
\tag{4}
$$

where γ_{tol} is the tolerance illustrating the maximum possible deviation from the desired main beam profile. Although the above optimization achieves the minimum power for the JRC system, it does not ensure the best antenna selection for the JRC operation because l_2-norm does not encourage sparsity. We can modify the above optimization to select the best $\bar{M}(< M)$ or fewer antennas in

8

the antenna array as follows:

$$
\begin{aligned}
\min_{\mathbf{w}_n} \quad & \|\mathbf{w}_n\|_2^2 \\
\text{subject to} \quad & |G_{\mathrm{rad}}e^{j\varphi(\theta_r)} - \mathbf{w}_n^{\mathrm{H}}\mathbf{a}(\theta_r)| \leq \gamma_{\mathrm{tol}}, \quad \theta_r \in \Theta_{\mathrm{rad}}, \\
& |\mathbf{w}_n^{\mathrm{H}}\mathbf{a}(\theta_\varepsilon)| \leq \varepsilon_{\mathrm{sl}}, \quad\quad\quad\quad\quad \theta_\varepsilon \in \Theta_{\mathrm{sl}}, \\
& \mathbf{w}_n^{\mathrm{H}}\mathbf{a}(\theta_c) = \Delta_{n,c}e^{j\phi_{n,c}}, \quad\quad\quad c = 1, \cdots, C, \\
& \|\mathbf{w}_n\|_0 \leq \bar{M}.
\end{aligned}
\tag{5}
$$

Instead of enforcing the hard sparsity constraint which allows the selection of a maximum of $\bar{M}$ antennas, l_0-penalty can be employed in the objective function to promote sparsity as follows:

$$
\begin{aligned}
\min_{\mathbf{w}_n} \quad & \|\mathbf{w}_n\|_2^2 + \eta\|\mathbf{w}_n\|_0 \\
\text{subject to} \quad & |G_{\mathrm{rad}}e^{j\varphi(\theta_r)} - \mathbf{w}_n^{\mathrm{H}}\mathbf{a}(\theta_r)| \leq \gamma_{\mathrm{tol}}, \quad \theta_r \in \Theta_{\mathrm{rad}}, \\
& |\mathbf{w}_n^{\mathrm{H}}\mathbf{a}(\theta_\varepsilon)| \leq \varepsilon_{\mathrm{sl}}, \quad\quad\quad\quad\quad \theta_\varepsilon \in \Theta_{\mathrm{sl}}, \\
& \mathbf{w}_n^{\mathrm{H}}\mathbf{a}(\theta_c) = \Delta_{n,c}e^{j\phi_{n,c}}, \quad\quad\quad c = 1, \cdots, C,
\end{aligned}
\tag{6}
$$

where η is the tuning parameter which controls the balance between the desired power optimization and the number of utilized antennas in the above multi-objective optimization. In optimization (6), the constraint handling the number of active antennas in optimization (5) is shifted to the objective function, i.e., (6) is a relaxed version of (5). In optimization (6), the value of $\bar{M}$ tends to decrease as the value of η increases. If η takes a very high value, the optimization problem (6) will only minimize the number of selected antennas irrespective of the power utilized by the antenna array. Note that for each selection of η, (6) provides a corresponding solution of $\bar{M}$ as well as the selected antennas for the beamforming vector $\mathbf{w}_n$. If this value of $\bar{M}$ obtained from (6) is used in the optimization problem (5), it will also potentially yield the same selected antennas for the beamforming weight vector. In this paper, we will only emphasize the optimization of problem (6).

Unfortunately, due to the non-convex nature of l_0-norm, the optimization (6) requires an exhaustive combinatorial search over all $\mathrm{C}_{\bar{M}}^M$ possible sparsity

9

patterns of $\mathbf{w}_n$, where the optimization (4) must be solved for each of these patterns. We can exploit l_1-norm which offers a close convex approximation of l_0-norm, albeit a weaker and indirect measure of sparsity [39], resulting in the following relaxed version of the optimization (6):

$$
\begin{aligned}
\min_{\mathbf{w}_n} \quad & \|\mathbf{w}_n\|_2^2 + \eta \|\mathbf{w}_n\|_1 \\
\text{subject to} \quad & |G_{\mathrm{rad}}e^{j\varphi(\theta_r)} - \mathbf{w}_n^{\mathrm{H}}\mathbf{a}(\theta_r)| \leq \gamma_{\mathrm{tol}}, \quad \theta_r \in \Theta_{\mathrm{rad}}, \\
& |\mathbf{w}_n^{\mathrm{H}}\mathbf{a}(\theta_\varepsilon)| \leq \varepsilon_{\mathrm{sl}}, \qquad\qquad \theta_\varepsilon \in \Theta_{\mathrm{sl}}, \\
& \mathbf{w}_n^{\mathrm{H}}\mathbf{a}(\theta_c) = \Delta_{n,c}e^{j\phi_{n,c}}, \qquad\quad c = 1, \cdots, C.
\end{aligned}
\tag{7}
$$

185   Here, it is important to consider the crucially defining difference between the l_0- and l_1-norm for our problem. The larger weights in $\mathbf{w}_n$ are penalized more heavily than the smaller weights in l_1-norm-based penalty. On the other hand, l_0-norm enforces democratized penalization which results in better sparse solutions because it penalizes all the non-zero weights of $\mathbf{w}_n$ equally. Therefore, the

190   optimization (7) is not an ideal formulation for antenna selection problem as the resulting solution might select more antennas than the exhaustive search-based optimization (6). To mollify this disparity, we exploit the re-weighted l_1-norm minimization, originally developed in the context of compressed sensing [39], to penalize the non-zero entries in $\mathbf{w}_n$ more democratically. Contrary to l_1-norm-

195   based relaxation where absolute values of all the beamforming coefficients are added, we must consider each coefficient as an independent parameter whose value, if selected, significantly improves the beamforming performance.

In order to enforce the democratic selection of antennas, we introduce a weighting function, inspired by [39], which counteracts the influence of beam-

200   forming coefficient magnitude in l_1-norm-based penalty as follows:

$$
u_{n,m} =
\begin{cases}
\dfrac{1}{|w_{n,m}|}, & \text{if } |w_{n,m}| > 0, \\
\dfrac{1}{\epsilon}, & \text{if } |w_{n,m}| = 0,
\end{cases}
\tag{8}
$$

where $w_{n,m}$ is mth $(m = 1, \ldots, M)$ coefficient in $\mathbf{w}_n$, and ϵ is a very small number. Thus, the weighting vector corresponding to the beamforming weight vector $\mathbf{w}_n$ can be represented as $\mathbf{u}_n = [u_{n,1}, u_{n,2}, \ldots, u_{n,M}]^{\mathrm{T}}$. If the optimal

10

solution $\mathbf{w}_n^{\text{opt}}$ of the optimization (6) is $\bar{M}$-sparse, i.e. $\|\mathbf{w}_n^{\text{opt}}\|_0 = \bar{M}$, the following optimization will tend to obtain the correct solution analogous to l_0-norm penalty in the optimization (6):

$$
\begin{aligned}
\min_{\mathbf{w}_n} \quad & \|\mathbf{w}_n\|_2^2 + \eta \left\| \mathbf{u}_n^{(i)} \odot \mathbf{w}_n \right\|_1 \\
\text{subject to} \quad & |G_{\text{rad}} e^{j\varphi(\theta_r)} - \mathbf{w}_n^{\text{H}} \mathbf{a}(\theta_r)| \le \gamma_{\text{tol}}, \quad \theta_r \in \Theta_{\text{rad}}, \\
& |\mathbf{w}_n^{\text{H}} \mathbf{a}(\theta_\varepsilon)| \le \varepsilon_{\text{sl}}, \qquad\qquad \theta_\varepsilon \in \Theta_{\text{sl}}, \\
& \mathbf{w}_n^{\text{H}} \mathbf{a}(\theta_c) = \Delta_{n,c} e^{j\phi_{n,c}}, \qquad\quad c = 1, \cdots, C.
\end{aligned}
\tag{9}
$$

The above optimization is executed iteratively and $\mathbf{u}^{(i)}$ denote the weights for the ith iteration. Such type of weighted optimization strategy is known to have a quick convergence [39]. We have observed the convergence of the algorithm in very few steps through simulations. The weighting vector $\mathbf{u}_n$ forces the small entries of the beamforming vector $\mathbf{w}_n$ to zero in the subsequent iteration. The small parameter ϵ, which should ideally be slightly smaller than the expected smallest non-zero magnitude of $\mathbf{w}_n$, provides stability and ensures that a zero-valued entry does not prohibit a non-zero estimate of the corresponding beamforming coefficient in the next step. The detailed algorithm for extracting the beamforming weight vectors is listed in Table I. This algorithm is employed for extracting all the desired N beamforming weight vectors individually.

Minimizing the total number of antennas for JRC may result in some spare hardware up-conversion chains which can be further used for other tasks. There

Table I: Transmit Antenna Selection for Individual Beamformers

Algorithm I: Transmit Antenna Selection for Individual Beamformers
1. *Initialize* the iteration count as $i = 0$ and the initial weight vector as $\mathbf{u}_n^{(0)} = \mathbf{1}_{M \times 1}$.
2. *Solve* the multi-objective re-weighted l_1-norm optimization problem (9).
3. *Increment* i and *update* the weighting vector $\mathbf{u}_n^{(i)}$ using Eq. (8).
4. *Terminate* on convergence or if the maximum number of iterations for i has reached; Otherwise, go to step 2.

are several ways to fully utilize all the available up-conversion chains. For example, a concurrent communication-only operation can be realized by the spare hardware chains to increase the communication data rate. Alternatively, as the final solution results in fewer than $\bar{M}$ activated antennas, we may turn on the remaining antennas based on the magnitude of the weighting coefficients. Note that the importance of each antenna is inversely proportional to the respective weighting $u_{n,m}$. If the optimal solution is achieved in the ith iteration, the most important antennas correspond to the elements of vector $\mathbf{u}_n^{(i)}$ which have the smallest amplitudes. Therefore, the $\bar{M}$ most important antennas can be identified by determining the $\bar{M}$ smallest elements in $|\mathbf{u}_n^{(i)}|$ and regenerating the beamforming weight vectors using the array manifold of those antennas by exploiting optimization (4). Another possible solution is to suspend the iterative optimization process once the desired number of antennas is achieved.

Our proposed iterative technique also falls in the general class of Majorization Minimization [40] algorithms where a surrogate function is exploited to achieve the optimal result. In our case, $\|\mathbf{u}_n \odot \mathbf{w}_n\|_1$ serves as the surrogate objective function of $\|\mathbf{w}_n\|_0$. In this sense, a wide variety of re-weighting techniques can be employed.

B. Joint Transmit Antenna Selection for Multiple Beamforming Vectors via Group-sparsity

The optimal selection of antennas discussed in Subsection III-A results in different antenna array configurations for different beamforming weight vectors. This is a serious disadvantage because frequent electronic switching of antennas needs to be performed using the fast switching circuitry whenever the beamforming weight vector is changed. For high data rates, this switching will become more frequent, resulting in an added complexity for the JRC system. It is also possible that although the antennas used by each beamformer are very less, practically all the antennas are being used. This happens when each antenna is used by at least one of the N beamformers. In such a scenario, the spare antennas cannot be used for any other purposes which is not an optimal

12

strategy when the additional radio transmission chains are still available.

We propose a joint optimal antenna selection strategy which optimizes the total number of transmit antennas used by all the beamformers for the JRC operation. For this purpose, the well-known group-sparsity concept [41] can be employed.

We define the mixed $l_{1,q}$-norm as:

$$\|\mathbf{w}\|_{1,q} := \sum_{m=1}^{M} \left(\sum_{n=1}^{N} |w_{n,m}|^q \right)^{1/q}, \tag{10}$$

which induces group-sparsity for $q > 1$ [42]. Recall that $w_{n,m}$ denotes the mth beamforming coefficient of $\mathbf{w}_n$. The most extensively used norms to enforce group-sparsity are $l_{1,2}$- and $l_{1,\infty}$-norms. For more detail, see [42].

Similar to the previous section, our proposed antenna selection strategy for grouped beamforming vectors takes the form of the following *joint* optimization:

$$\min_{\mathbf{w}_n} \quad \sum_{n=1}^{N} \|\mathbf{w}_n\|_2^2 + \eta \|\mathbf{w}\|_{1,q}$$

subject to $\quad |G_{\mathrm{rad}} e^{j\varphi(\theta_r)} - \mathbf{w}_n^{\mathrm{H}} \mathbf{a}(\theta_r)| \leq \gamma_{\mathrm{tol}}, \ \theta_r \in \Theta_{\mathrm{rad}}; \ n = 1, \ldots, N,$ (11)

$$|\mathbf{w}_n^{\mathrm{H}} \mathbf{a}(\theta_\varepsilon)| \leq \varepsilon_{\mathrm{sl}}, \ \theta_\varepsilon \in \Theta_{\mathrm{sl}}; \ n = 1, \ldots, N,$$

$$\mathbf{w}_n^{\mathrm{H}} \mathbf{a}(\theta_c) = \Delta_{n,c} e^{j\phi_{n,c}}, \ c = 1, \cdots, C; \ n = 1, \ldots, N.$$

Note that contrary to the optimization (7) which is exploited for each beamforming weight vector separately, the optimization (11) jointly solves all the beamforming vectors simultaneously. Moreover, the optimization (11) yields the beamforming weight vectors which exploit the same antenna elements for the JRC operation but have different weights depending on their sidelobe communication profile.

In continuation of our discussion in the previous section regarding sparsity enhancement, the group-sparsity can also be significantly enhanced democrati-

cally by exploiting a similar weighting function as in (8) as follows:

$$v_m = \begin{cases} \dfrac{1}{\left(\displaystyle\sum_{n=1}^{N} |w_{n,m}|^q\right)^{1/q}}, & \text{if } \displaystyle\sum_{n=1}^{N} |w_{n,m}| > 0, \\[3ex] \dfrac{1}{\epsilon}, & \text{if } \displaystyle\sum_{n=1}^{N} |w_{n,m}| = 0. \end{cases} \qquad (12)$$

The resulting optimization employing group sparsity which enables optimal antenna selection jointly for all the beamforming weight vectors can now be expressed as follows:

$$\min_{\mathbf{w}_n} \quad \sum_{n=1}^{N} \|\mathbf{w}_n\|_2^2 + \eta \sum_{m=1}^{M} \left(v_m^{(i)} \sum_{n=1}^{N} |w_{n,m}|^q \right)^{1/q}$$

$$\text{subject to} \quad |G_{\text{rad}} e^{j\varphi(\theta_r)} - \mathbf{w}_n^{\text{H}} \mathbf{a}(\theta_r)| \leq \gamma_{\text{tol}}, \ \theta_r \in \Theta_{\text{rad}}; \ n = 1, \dots, N, \qquad (13)$$

$$|\mathbf{w}_n^{\text{H}} \mathbf{a}(\theta_\varepsilon)| \leq \varepsilon_{\text{sl}}, \ \theta_\varepsilon \in \Theta_{\text{sl}}; \ n = 1, \dots, N,$$

$$\mathbf{w}_n^{\text{H}} \mathbf{a}(\theta_c) = \Delta_{n,c} e^{j\phi_{n,c}}, \ c = 1, \cdots, C; \ n = 1, \dots, N,$$

where the above optimization is solved iteratively and $v_m^{(i)}$ denotes the weighting coefficient for the ith iteration. This multi-objective optimization strategy tends to provide the antenna array design for the JRC operation which ensures the selection of the least number of transmit antennas and minimizes their power utilization. The detailed algorithm for extracting the beamforming weight vectors using this approach is listed in Table II.

It is interesting to note that both proposed iterative algorithms for optimal antenna selection and power optimization iteratively solve a convex optimization problem, whereas the overall algorithm does not. Instead, the overall iterative strategy forces one part of the objective function to find a local minimum of a non-convex penalty function that resembles l_0-norm for antenna selection through re-weighted l_1-norm. Moreover, the other part of the objective function tends to minimize the power utilization of the selected antennas.

Group sparsity-based approach will utilize more number of antennas than individual beamforming weight vector at a given fast time. However, due to an-

14

Table II: Transmit Antenna Selection for Grouped Beamformers by Employing Group Sparsity

Algorithm II: Transmit Antenna Selection for Grouped Beamformers
1. *Initialize* the iteration count as $i = 0$ and the initial weight vector as $v_m^{(0)} = 1$.
2. *Solve* the multi-objective re-weighted $l_{1,2}$-norm-based joint optimization (11).
3. *Increment* i and *update* the weighting $v_m^{(i)}$ using Eq. (12).
4. *Terminate* on convergence or if the maximum number of iterations for i has reached; Otherwise, go to step 2.

tenna switching, the total number of antennas used by individual beamforming weight vectors are generally more than group sparse version in slow time.

IV. Comparative Analysis of the Proposed Strategies

Let us compare the antenna selection by individual beamformer design (9) and group sparsity-based beamformer design (13). The most important difference between the two schemes lies in that the group sparsity-based approach (13) extracts the optimal antennas for all beamformers which not only satisfy the radar tasks but also enable transmission of all the given set of communication symbols to all communication users. On the other hand, the individual beamformer design strategy only selects the optimal antenna positions which satisfy the radar tasks and can transmit only one respective communication symbol to each communication receiver, i.e., only one beamformer is designed at a time (9).

Note that the constraints of the maximum allowable sidelobe level and the radar main beam tolerance are common for both schemes (9) and (13). The only difference lies in the communication constraints. The optimization (9) has C equality constraints corresponding to the communication operation because this approach designs only one beamforming weight vector at a time which

15

serves one communication symbol to each communication receiver. On the other hand, (13) has NC communication constraints as this approach designs all the N beamforming weight vectors simultaneously which can further be used to deliver all the possible communication information to the communication users. Since (13) has more constraints than (9), it will generally tend to select more antennas than (9) to satisfy all those constraints. However, to deliver all the possible communication information to all the communication users, optimization (9) is executed N times to generate N beamforming weight vectors which can achieve such task. Optimization (9) generally results in different antenna selections for different beamforming weight vectors. In this case, the overall number of antennas used by (9) to produce all the desired beamforming weight vectors will likely exceed the number of antennas selected by (13). Moreover, (9) will require frequent antenna switching for different slow times whenever communication information being transmitted is changed. Therefore, the proposed group sparsity-based approach (13) is preferred for antenna selection as it requires fewer number of antennas and prevents frequent antenna switching, thereby easing the hardware implementation.

For a given number of hardware chains $\bar{M}$, the total number of feasible antenna configurations is given by:

$$U_{\text{count}} = \text{C}_{\bar{M}}^{M}, \tag{14}$$

Therefore, an exhaustive search will require us to evaluate the feasibility of U_{count} number of array configurations to achieve the optimal solution. On the other hand, if the antennas are randomly selected, the probability to achieve the optimal solution will be:

$$P_{\text{opt}} = \frac{1}{U_{\text{count}}} = \frac{1}{\text{C}_{\bar{M}}^{M}}. \tag{15}$$

Note that the array configuration obtained from random antenna selection may not satisfy the radar and communication objectives. Therefore, it is impractical to use random selection or exhaustive search to obtain the desired array configuration.

V. Simulation Results

In this section, we present simulation results to illustrate the performance of the proposed antenna selection strategy for the beamforming-based JRC system. In all the simulations, we consider a uniform linear array (ULA) consisting of $M = 30$ transmit antennas to optimize the radar main beam objectives and serve two ($C = 2$) communication users located in the sidelobe region of the radar at angles 30° and 40°, respectively. We set the inter-sensor spacing of the ULA at 0.25λ and the tuning coefficient η for all the multi-objective optimizations is set to unity. The maximum allowable sidelobe level for all the cases is considered to be lower than $\varepsilon_{\mathrm{sl}} = -20$ dB. We use the open-source SDPT3 solver [43] integrated with the open-source version of CVX toolbox [44] to solve all the optimizations. For the simulations involving the focused beampattern, the JRC radar objective is to focus the main beam with a gain of 0 dB at $\theta_r = 0°$. For flat-top beampattern synthesis experiments, the radar objective is to project the main beam with a gain of 0 dB for angles from $-7°$ to $7°$. For this purpose, we consider Θ_{sl} consisting of a grid of angles with a grid spacing of 0.5°. The value of $q = 2$ for the group-sparse optimization (13), i.e. mixed $l_{1,2}$-norm is used.

A. Convergence analysis for individual beampattern synthesis

First, we consider the beampattern synthesis for the radar main beam focused at $\theta_r = 0°$ using Algorithm I. In this scenario, the JRC system aims to project an amplitude of -20 dB towards both communication receivers. Fig. 3(a) demonstrates the power distribution profile of the beamforming weight vector synthesized using Algorithm I. The corresponding number of selected antennas during each iteration of Algorithm I is illustrated in Fig. 3(b). Moreover, Fig. 3(c) shows the spatial selection profile during each iteration of the Algorithm I for the first 4 iterations.
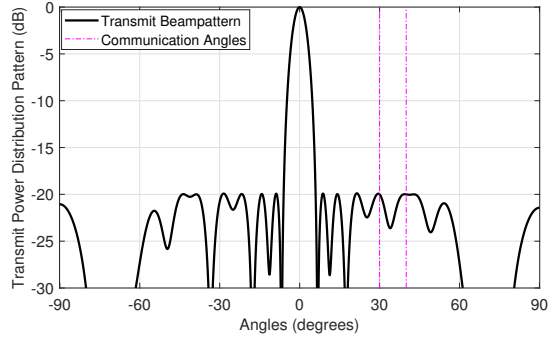
(a)
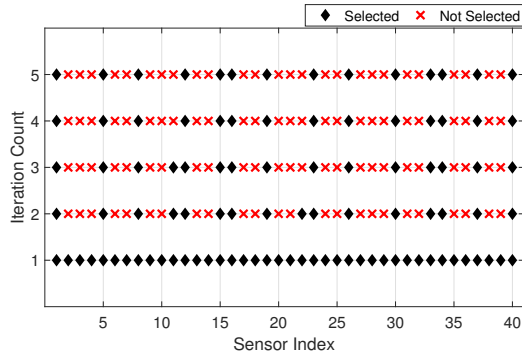
(b)
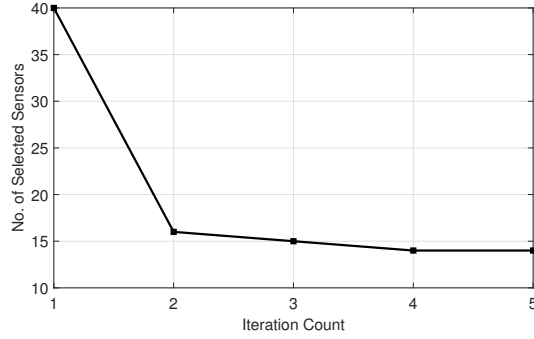
(c)

Figure 3: Focused beampatterns synthesis using the optimal antenna selection strategy in Algorithm I ($M = 40, \Theta_{\mathrm{rad}} = 0^\mathrm{o}, \Theta_{\mathrm{trans}} = [-6^\mathrm{o}\ 0^\mathrm{o}) \cup (0^\mathrm{o}\ 6^\mathrm{o}], \Theta_{\mathrm{sl}} = [-90^\mathrm{o}\ -6^\mathrm{o}) \cup (6^\mathrm{o}\ 90^\mathrm{o}], G_{\mathrm{rad}} = 1, \gamma_{\mathrm{tol}} = 10^{-3}, \varepsilon_{\mathrm{sl}} = 0.1$ (20 dB below G_{rad}): (a) Transmit power distribution pattern, (b) Total number of selected antennas w.r.t the number of iterations, (c) Spatial antenna selection profile for each iteration.

It can be observed that the algorithm converges very fast, i.e. only 4 iterations were enough to achieve the final solution. It can also be observed that the spatial profile of the selected antennas does not change after the convergence. Moreover, we also ran the Algorithm I for up to 100 iterations but did not observe any change in the spatial antenna selection profile.

Fig. 4 illustrates the similar results for flat-top beampattern synthesis. In Fig. 4(a), we observe the synthesized beampatten derived from Algorithm I and note that it achieves both radar and communication objectives. The corresponding number of selected antennas during each iteration is shown in Fig. 4(b). It can be observed that the Algorithm I converged within 4 iterations. We extended the iteration count up to 100 iterations and noted that the spatial antenna selection profile, as shown in Fig. 4(c) illustrating the selection of 14 antennas, did not change after the first 4 iterations.

If the optimal number of antennas is known to be 14, an exhaustive search will require us to evaluate $C_{14}^{40} \approx 2 \times 10^{10}$ different configurations of antennas which is impractical. If the optimal number of antennas is unknown, exhaustive search will require us to evaluate $\sum_{m=1}^{40} C_{m}^{40}$ possible array configurations.

B. Antenna selection for individual beamforming weight vectors

Now we discuss the set of beampatterns that have the same main beam profile but transmit different communication information. Without loss of generality, we consider the 2-ASK multiple-access signaling scheme where the JRC transmit array has an objective to transmit two (same or different) amplitude levels towards both communication receivers. This results in four different combinations of possible beampatterns.
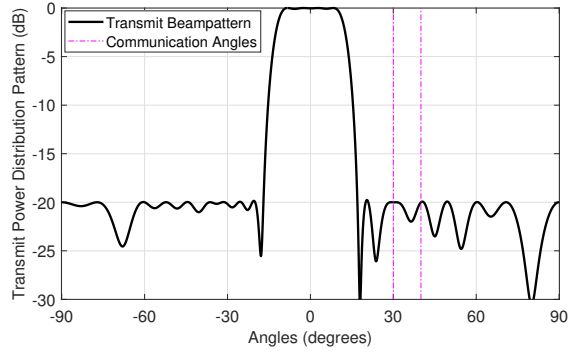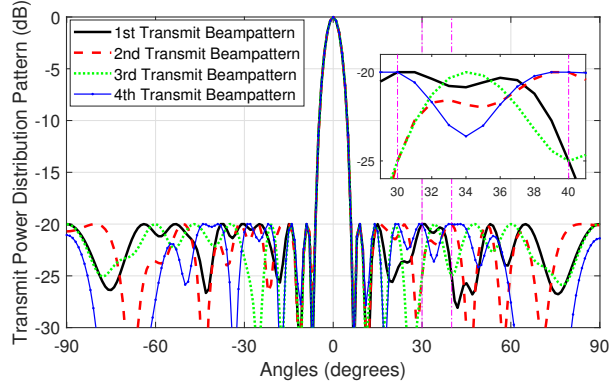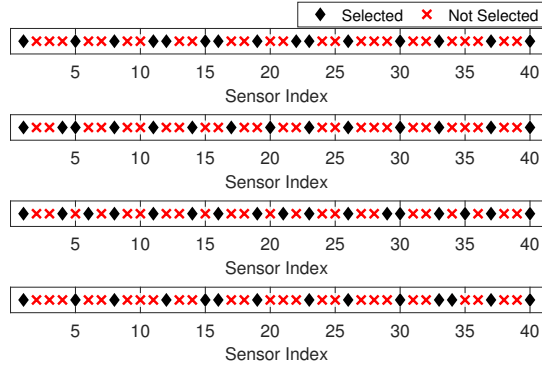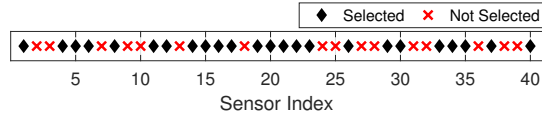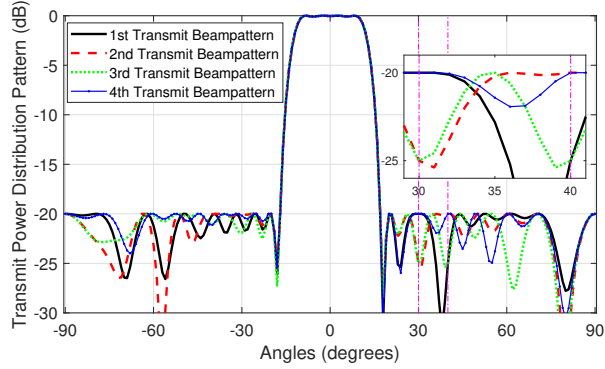
(a)
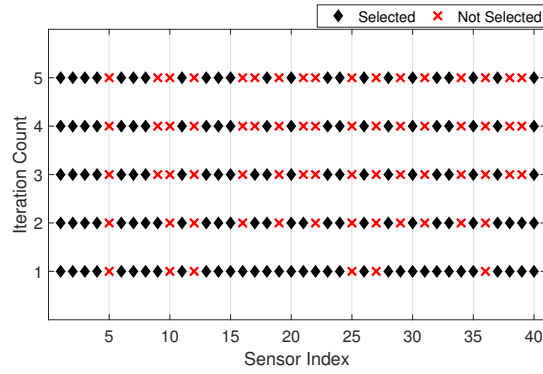
(b)
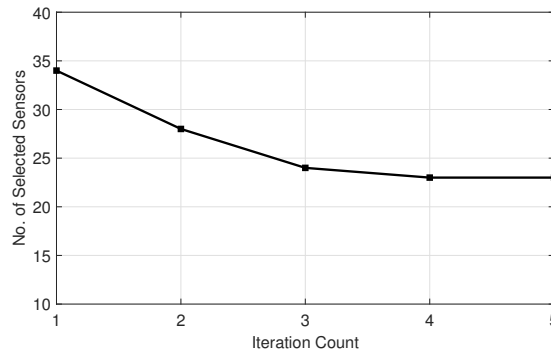
(c)

Figure 4: Flat-top beampattern synthesis using the antenna selection strategy in Algorithm I ($M = 40, \Theta_{\mathrm{rad}} = [-7^{\mathrm{o}} \ \ 7^{\mathrm{o}}]$, $\Theta_{\mathrm{trans}} = [-17^{\mathrm{o}} \ \ -7^{\mathrm{o}}) \cup (7^{\mathrm{o}} \ \ 17^{\mathrm{o}}]$, $\Theta_{\mathrm{sl}} = [-90^{\mathrm{o}} \ \ -17^{\mathrm{o}}) \cup (17^{\mathrm{o}} \ \ 90^{\mathrm{o}}], G_{\mathrm{rad}} = 1, \gamma_{\mathrm{tol}} = 10^{-3}, \varepsilon_{\mathrm{sl}} = 0.1$ (20 dB below G_{rad}): (a) Transmit power distribution pattern, (b) Total number of selected antennas w.r.t the number of iterations, (c) Spatial antenna selection profile with increasing number of iterations

20

(a)

(b)

(c)

Figure 5: Focused beampattern synthesis using the antenna selection strategy in Algorithm I for different communication objectives ($M = 40, \Theta_{\mathrm{rad}} = 0^{\mathrm{o}}$, $\Theta_{\mathrm{trans}} = [-6^{\mathrm{o}}\ 0^{\mathrm{o}}) \cup (0^{\mathrm{o}}\ 6^{\mathrm{o}}]$, $\Theta_{\mathrm{sl}} = [-90^{\mathrm{o}}\ -6^{\mathrm{o}}) \cup (6^{\mathrm{o}}\ 90^{\mathrm{o}}], G_{\mathrm{rad}} = 1, \gamma_{\mathrm{tol}} = 10^{-3}, \varepsilon_{\mathrm{sl}} = 0.1$ (20 dB below G_{rad}) : (a) Transmit power distribution pattern, (b) Final antenna selection profile for each beampattern, (c) Overall antenna selection profile containing the antennas selected at least once by any of the beamforming weight vectors.

21

Using Algorithm I, we synthesized the focused beampatterns for the JRC system as illustrated in Fig. 5(a). The final spatial optimal antenna selection profile for these respective beamformers is shown in Fig. 5(b). It can be observed that the number of antennas used for each beampattern is not the same. Note that a maximum of 17 antennas will be exploited by any of the beamformers at a given time. Fig. 5(c) shows all the individual antennas which are selected at least once by the respective four beampatterns. It shows that the overall number of antennas collectively used by all the beamformers is 24. This means that 24 antennas will remain in operation by the JRC system, which is more than the number of antennas individually required by each beamformer. Extensive antenna switching will be also be required inviting hardware complexity.

Similar results have been obtained for the flat-top beampattern synthesis, shown in Fig. 6(a), using the Algorithm I by exploiting 2-ASK signaling strategy. It can be observed from Fig. 6(b) that the four beamformers exploit 21, 21, 20, and 23 antennas, respectively. However, the total number of antennas used by all the beamformers collectively is 36 as shown in Fig 6. This signifies our previous analysis that the antenna array utilization might be sub-optimal if the beamforming weight vectors are synthesized individually.

C. Antenna Selection by Employing Group Sparsity

The simulation results from Subsection V-B motivate to inspect the optimal antenna selection performance for a group of beamforming weight vectors collectively. We exploit the same scenario as in Subsection V-B where 2-ASK signaling strategy is exploited. We find the optimal antenna selection for a group of four beamforming weight vectors using the group-sparsity Algorithm II which satisfies radar and communication objectives simultaneously.

22

(a)
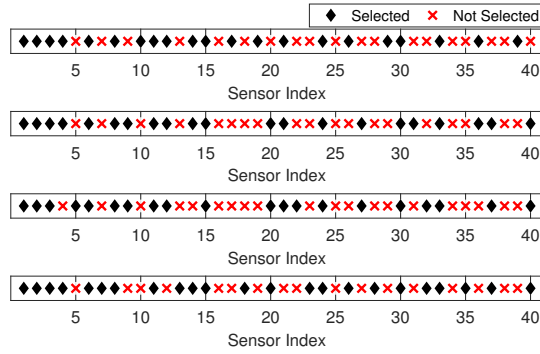
(b)
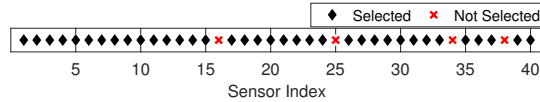
(c)

Figure 6: Flat-top beampattern synthesis using the antenna selection strategy in Algorithm I for different communication objectives ($M = 40, \Theta_{\mathrm{rad}} = [-7^{\mathrm{o}}\ 7^{\mathrm{o}}]$, $\Theta_{\mathrm{trans}} = [-17^{\mathrm{o}}\ -7^{\mathrm{o}}) \cup (7^{\mathrm{o}}\ 17^{\mathrm{o}}]$, $\Theta_{\mathrm{sl}} = [-90^{\mathrm{o}}\ -17^{\mathrm{o}}) \cup (17^{\mathrm{o}}\ 90^{\mathrm{o}}]$, $G_{\mathrm{rad}} = 1, \gamma_{\mathrm{tol}} = 10^{-3}, \varepsilon_{\mathrm{sl}} = 0.1$ (20 dB below G_{rad}): (a) Transmit power distribution pattern, (b) Final antenna selection profile for each beampattern, (c) Overall antenna selection profile containing the antennas selected at least once by any of the beamforming weight vectors.
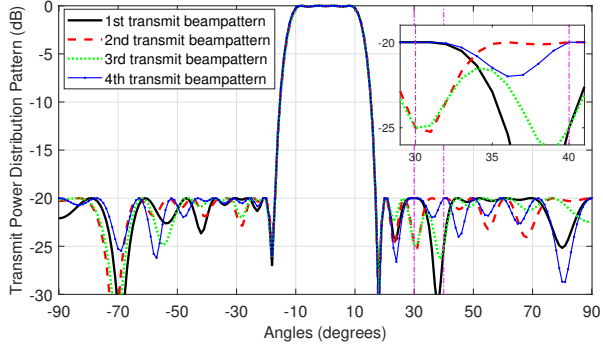
23
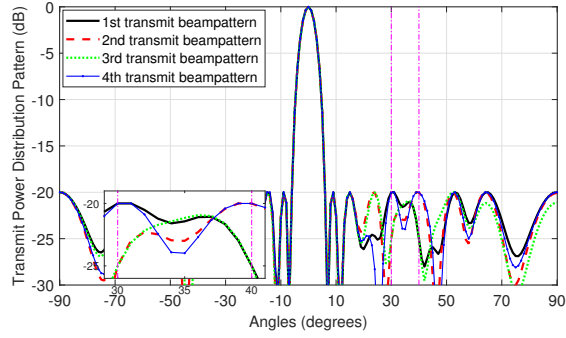
(a)
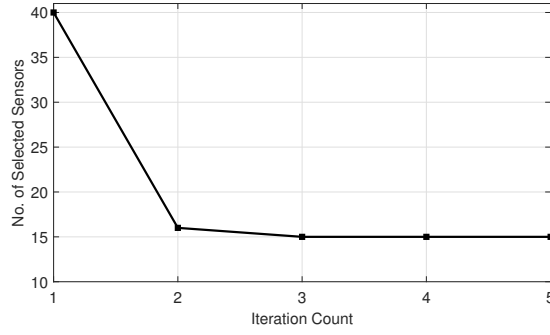
(b)
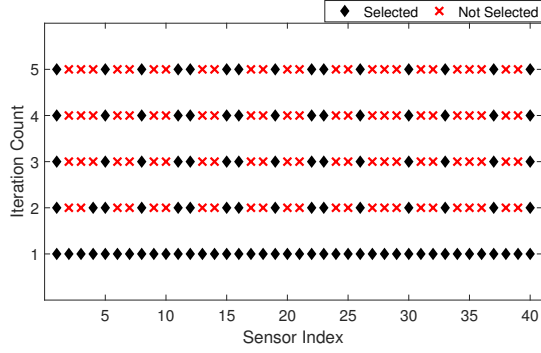
(c)

Figure 7: Focused beampattern synthesis by employing the group-sparsity for antenna selection Algorithm II ($M = 40, \Theta_{\mathrm{rad}} = 0^{\mathrm{o}}$, $\Theta_{\mathrm{trans}} = [-6^{\mathrm{o}}\ 0^{\mathrm{o}}) \cup (0^{\mathrm{o}}\ 6^{\mathrm{o}}]$, $\Theta_{\mathrm{sl}} = [-90^{\mathrm{o}}\ -6^{\mathrm{o}}) \cup (6^{\mathrm{o}}\ 90^{\mathrm{o}}], G_{\mathrm{rad}} = 1, \gamma_{\mathrm{tol}} = 10^{-3}, \varepsilon_{\mathrm{sl}} = 0.1(20$ dB below $G_{\mathrm{rad}})$: (a) Transmit power distribution pattern, (b) Number of selected antennas with increasing number of iterations, (c) Spatial antenna selection profile for the first 5 iterations.

Fig. 7(a) shows the power distribution pattern of the four beamforming weight vectors for the focused main beam synthesized by using Algorithm II. Note that in this approach, all the beamforming weight vectors exploit the same antenna array elements. Contrary to the results using Algorithm I in Fig. 5(c), where an overall 24 antennas of the JRC transmit array are used, Figs. 7(b)-(c) show that the grouped approach exploits only 15 antennas. Fig. 7(b) shows the number of selected antennas with the increasing number of iterations. Note that the Algorithm II converged within 3 iterations.

A similar result has been observed for the flat-top beampattern synthesis in Fig. 8 using group-sparsity Algorithm II. Fig. 8(a) shows the power distribution pattern for the four beamforming weight vectors resulting from Algorithm II. It can be observed that all the beampatterns satisfy the radar and communication objectives. Contrary to Fig. 6, where 36 antenna elements were selected at least once by the beamforming vectors, Fig. 8 shows that only 21 antennas are exploited when all the beamforming vectors were extracted simultaneously as a group using the Algorithm II. Fig. 8(b) shows the number of selected antennas with the increasing number of iterations. It can be observed that the Algorithm II converged within 4 iterations. The corresponding spatial antenna selection profile is illustrated in Fig. 8(c).

It has been observed that when the beamforming weight vectors are derived simultaneously as a group, they exploit overall fewer number of antennas compared to the case when the beamforming weight vectors are synthesized individually. These results show a significant advantage of utilizing Algorithm II. In such a scenario, the additional antennas can be exploited to perform other objectives. Moreover, the grouped antenna selection-based strategy prevents frequent antenna switching when the beamforming weights are changed, which eases the implementation of the JRC system. The fast convergence of the proposed algorithms also emphasizes their importance.
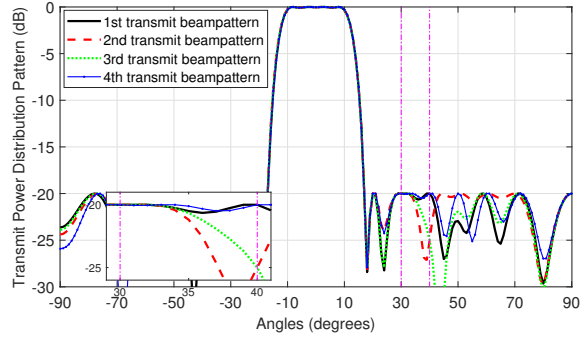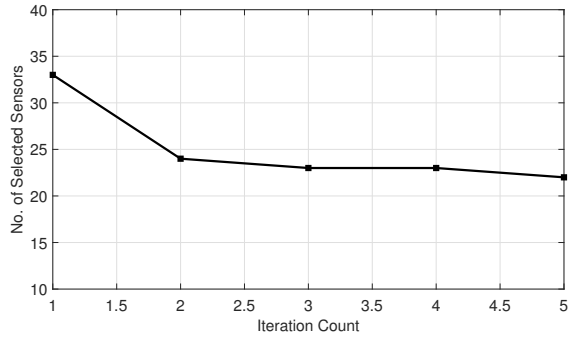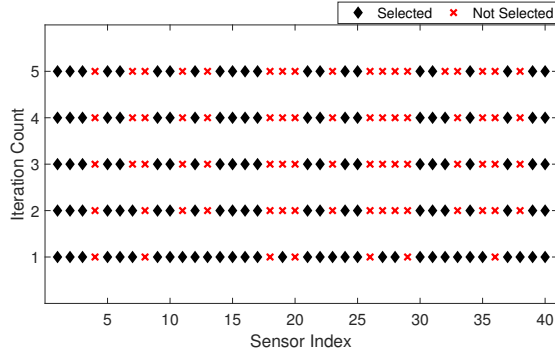
(a)
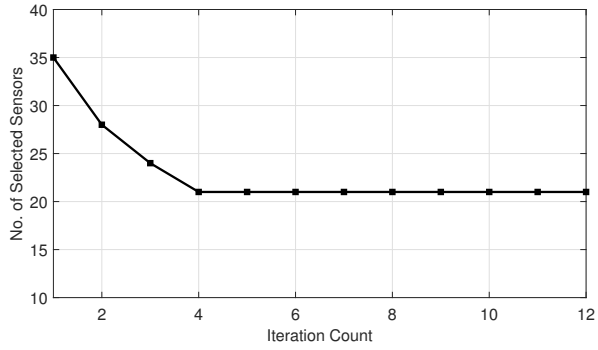
(b)
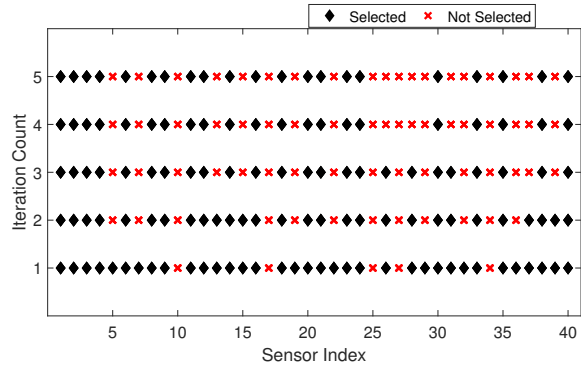
(c)

Figure 8: Flat-top beampattern synthesis by employing the group-sparsity based antenna selection Algorithm II ($M = 40, \Theta_{\mathrm{rad}} = [-7^{\mathrm{o}} \ \ 7^{\mathrm{o}}]$, $\Theta_{\mathrm{trans}} = [-17^{\mathrm{o}} \ \ -7^{\mathrm{o}}) \cup (7^{\mathrm{o}} \ \ 17^{\mathrm{o}}]$, $\Theta_{\mathrm{sl}} = [-90^{\mathrm{o}} \ \ -17^{\mathrm{o}}) \cup (17^{\mathrm{o}} \ \ 90^{\mathrm{o}}], G_{\mathrm{rad}} = 1, \gamma_{\mathrm{tol}} = 10^{-3}, \varepsilon_{\mathrm{sl}} = 0.1$ (20 dB below G_{rad}): (a) Transmit power distribution pattern, (b) Number of selected antennas with increasing number of iterations, (c) Spatial antenna selection profile for the first 5 iterations.

26

(a)

(b)

(c)

Figure 9: Flat-top beampattern synthesis by employing the group-sparsity based antenna selection Algorithm II using QAM-based sidelobe modulation ($M = 40, \Theta_{\mathrm{rad}} = [-7^{\mathrm{o}} \ 7^{\mathrm{o}}]$, $\Theta_{\mathrm{trans}} = [-17^{\mathrm{o}} \ -7^{\mathrm{o}}) \cup (7^{\mathrm{o}} \ 17^{\mathrm{o}}]$, $\Theta_{\mathrm{sl}} = [-90^{\mathrm{o}} \ -17^{\mathrm{o}}) \cup (17^{\mathrm{o}} \ 90^{\mathrm{o}}], G_{\mathrm{rad}} = 1, \gamma_{\mathrm{tol}} = 10^{-3}, \varepsilon_{\mathrm{sl}} = 0.1$ (20 dB below G_{rad}): (a) Transmit power distribution pattern for the first four beampatterns, (b) Number of selected antennas with increasing number of iterations, (c) Spatial antenna selection profile for the first 5 iterations.
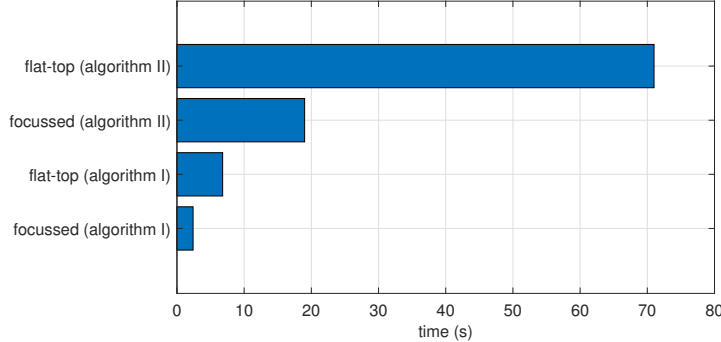
27

Figure 10: Computation time required to compute the beamforming weight vectors using the proposed approaches.

D. Computation Time

Now we compare the computation time for both proposed antenna selection algorithms outlined in Tables I and II. Fig. 10 illustrates the run-time of generating all the required beamforming weight vectors in Figs. 5–8. For these simulations, we used a computer equipped with Intel(R) Core(TM) i7-6700 processor, 16 GB DDR3 (1600 MHz) RAM, 64-bit Windows 8.1 Enterprise, and MATLAB R2017b (64-bit). It can be observed that the group sparsity-based antenna selection strategy takes longer computation time as compared to the antenna selection strategy developed for individual beamformers. This is expected from the formulation of both strategies as the group sparsity-based approach exploits l_2-norm of all the beamforming weight vectors during the optimization as well as for computing the weighting coefficients.

E. Antenna Selection for QAM-based Sidelobe Modulation

Now we modify the parameters used in Fig. 8 to investigate the antenna selection performance for QAM-based sidelobe modulation by employing two possible phases for each communication user. We find the optimal antenna selection for a group of sixteen beamforming weight vectors using the group sparsity-based Algorithm II which satisfies radar and communication objectives simultaneously.

28

Fig. 9(a) shows the power distribution pattern of the first four beamforming weight vectors for the flat-top main beam synthesized by using Algorithm II. All the beamformers exploit the same antenna array elements. Contrary to Fig. 8 where 21 antenna elements are selected, Fig. 9 shows that 22 antennas are exploited. Although the QAM-based signaling increased the number of required beamforming weight vectors from 4 to 16, only one additional antenna was required to satisfy the radar and communication objectives compared to 2-ASK signaling.

F. Antenna Selection for Randomly Located Communication Users

In this simulation, we investigate the performance of the group sparsity-based antenna selection approach for the case where communication users are randomly located in the sidelobe region. We use the same simulation parameters as in Fig. 9, but communication user locations are randomly selected such that they do not lie within the radar main beam and their angular separation is at least 10°. We perform 500 Monte Carlo trials for this case and the simulation results are presented in Fig. 11. Note that the antenna utilization count is very low for most of the simulation experiments. High antenna utilization is observed for the cases when the communication users are either very close to the radar main beam, or very close to 90° or -90°. This is because the JRC transmit array requires more degrees-of-freedom to satisfy all the constraints for those cases.
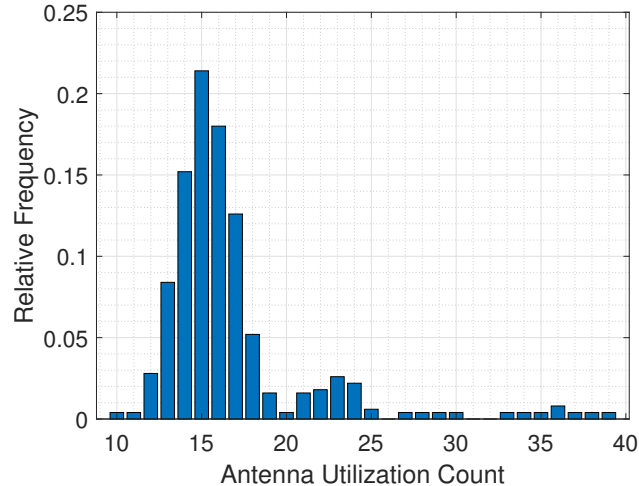
Figure 11: Relative frequency of antenna utilization for randomly generated simulation events.

VI. Conclusion

In this paper, we present a novel antenna selection strategy for JRC operation. We formulate a multi-objective optimization framework that aims to select the least possible number of antennas for the beamforming-based JRC system and minimize their respective power consumption. We show that the desired sparsity levels for antenna selection can be achieved for individual beamformers, as well as for the group of beamformers by using the same set of antennas. Simulation results illustrate that the proposed approach significantly reduces the number of antennas required to meet the prescribed service level for radar and communication operations. Furthermore, the performance of the proposed approach is analogous to that of l_0-norm-based exhaustive search optimization at a significantly reduced computational complexity.

References

[1] A. Ahmed, S. Zhang, Y. D. Zhang, Optimized sensor selection for joint radar-communication systems, in: Proc. IEEE Int. Conf. on Acoustics, Speech, and Signal Process., Barcelona, Spain, 2020.

[2] C. Sturm, T. Zwick, W. Wiesbeck, An OFDM system concept for joint radar and communications operations, in: Proc. IEEE Veh. Technol. Conf., Barcelona, Spain, 2009.

[3] S. D. Blunt, M. R. Cook, J. Stiles, Embedding information into radar emissions via waveform implementation, in: Proc. Waveform Diversity and Design Conf., Niagara Falls, Canada, 2010, pp. 195–199. `doi:10.1109/WDD.2010.5592502`.

[4] H. Griffiths, S. Blunt, L. Cohen, L. Savy, Challenge problems in spectrum engineering and waveform diversity, in: Proc. IEEE Radar Conf., Ottawa, Canada, 2013, pp. 1–5. `doi:10.1109/RADAR.2013.6586140`.

[5] H. Deng, B. Himed, Interference mitigation processing for spectrum-sharing between radar and wireless communications systems, IEEE Trans. Aerosp. Electron. Syst. 49 (3) (2013) 1911–1919. `doi:10.1109/TAES.2013.6558027`.

[6] A. Hassanien, M. G. Amin, Y. D. Zhang, F. Ahmad, Signaling strategies for dual-function radar communications: An overview, IEEE Aerosp. Electron. Syst. Mag. 31 (10) (2016) 36–45. `doi:10.1109/MAES.2016.150225`.

[7] S. D. Blunt, J. G. Metcalf, C. R. Biggs, E. Perrins, Performance characteristics and metrics for intra-pulse radar-embedded communication, IEEE J. Sel. Areas in Commun. 29 (10) (2011) 2057–2066. `doi:10.1109/JSAC.2011.111215`.

[8] D. W. Bliss, Cooperative radar and communications signaling: The estimation and information theory odd couple, in: Proc. IEEE Radar Conf., Cincinnati, OH, 2014, pp. 50–55. `doi:10.1109/RADAR.2014.6875553`.

[9] H. T. Hayvaci, B. Tavli, Spectrum sharing in radar and wireless communication systems: A review, in: Proc. Int. Conf. Electromagn. in Advanced Appl., Palm Beach, Aruba, 2014, pp. 810–813. `doi:10.1109/ICEAA.2014.6903969`.

[10] J. Euzire, R. Guinvarc'h, M. Lesturgie, B. Uguen, R. Gillard, Dual function radar communication time-modulated array, in: Proc. Int. Radar Conf., Lille, France, 2014, pp. 1–4. `doi:10.1109/RADAR.2014.7060416`.

[11] Z. Geng, H. Deng, B. Himed, Adaptive radar beamforming for interference mitigation in radar-wireless spectrum sharing, IEEE Signal Process. Lett. 22 (4) (2015) 484–488. `doi:10.1109/LSP.2014.2363585`.

[12] K. W. Huang, M. Bic, U. Mitra, V. Koivunen, Radar waveform design in spectrum sharing environment: coexistence and cognition, in: Proc. IEEE Radar Conf., Arlington, VA, 2015, pp. 1698–1703.

[13] J. R. Guerci, R. M. Guerci, A. Lackpour, D. Moskowitz, Joint design and operation of shared spectrum access for radar and communications, in: Proc. IEEE Radar Conf., Arlington, VA, 2015, pp. 761–766. `doi:10.1109/RADAR.2015.7131098`.

[14] D. Ciuonzo, A. De Maio, G. Foglia, M. Piezzo, Intrapulse radar-embedded communications via multiobjective optimization, IEEE Trans. Aerosp. Electron. Syst. 51 (4) (2015) 2960–2974. `doi:10.1109/TAES.2015.140821`.

[15] A. Hassanien, M. G. Amin, Y. D. Zhang, F. Ahmad, Dual-function radar-communications: Information embedding using sidelobe control and waveform diversity, IEEE Trans. Signal Process. 64 (8) (2016) 2168–2181. `doi:10.1109/TSP.2015.2505667`.

[16] A. Hassanien, M. G. Amin, Y. D. Zhang, F. Ahmad, Phase-modulation based dual-function radar-communications, IET Radar, Sonar & Navigation 10 (8) (2016) 1411–1421. `doi:10.1049/iet-rsn.2015.0484`.

[17] Y. Liu, G. Liao, J. Xu, Z. Yang, Y. Zhang, Adaptive OFDM integrated radar and communications waveform design based on information theory, IEEE Commun. Lett. 21 (10) (2017) 2174–2177.

[18] A. Ahmed, Y. D. Zhang, B. Himed, Multi-user dual-function radar-communications exploiting sidelobe control and waveform direversity, in: Proc. IEEE Radar Conf., Oklahoma City, OK, 2018.

[19] A. Ahmed, Y. Gu, D. Silage, Y. D. Zhang, Power-efficient multi-user dual-function radar-communication, in: Proc. IEEE Int. Workshop Signal Process. Advances in Wireless Commun., Kalamata, Greece, 2018, pp. 1–5.

[20] A. Ahmed, Y. D. Zhang, Y. Gu, Dual-function radar-communications using QAM-based sidelobe modulation, Digital Signal Process. 82 (2018) 166–174.

[21] I. P. Eedara, A. Hassanien, M. G. Amin, B. D. Rigling, Ambiguity function analysis for dual-function radar communications using PSK signaling, in: Proc. Asilomar Conf. Signals, Systems, and Computers, 2018, pp. 900–904.

[22] M. Bica, V. Koivunen, Radar waveform optimization for target parameter estimation in cooperative radar-communications systems, IEEE Trans. Aerosp. Electron. Syst.`doi:10.1109/TAES.2018.2884806`.

[23] S. Zhang, Y. Gu, Y. D. Zhang, Robust astronomical imaging in the presence of radio frequency interference, J. Astronom. Instrument. 8 (1) (2019) 1–15.

[24] M. Bica, V. Koivunen, Multicarrier radar-communications waveform design for RF convergence and coexistence, in: Proc. IEEE Int. Conf. Acoust., Speech, Signal Process., Brighton, U.K., 2019, pp. 7780–7784.

[25] A. Ahmed, Y. D. Zhang, B. Himed, Distributed dual-function radar-communication MIMO system with optimized resource allocation, in: Proc. IEEE Radar Conf., Boston, MA, 2019.

[26] A. Dimas, M. A. Clark, B. Li, K. Psounis, A. P. Petropulu, On radar privacy in shared spectrum scenarios, in: Proc. IEEE Int. Conf. Acoust., Speech, Signal Process., Brighton, U.K., 2019, pp. 7790–7794.

[27] A. Ahmed, S. Zhang, V. S. Amin, Y. D. Zhang, Spectrum sharing strategy for radio frequency based medical services, in: Proc. IEEE Signal Process. in Medicine and Biology Symp., Philadelphia, PA, 2019.

[28] A. Ahmed, Y. D. Zhang, A. Hassanien, B. Himed, OFDM-based joint radar-communication system: Optimal sub-carrier allocation and power distribution by exploiting mutual information, in: Proc. Asilomar Conf. Signals, Systems, and Computers, Pacific Grove, CA, 2019.

[29] A. Ahmed, D. Silage, Y. D. Zhang, Chance constrained beamforming for joint radar-communication systems, in: Proc. IEEE Sensor Array and Multichannel Signal Process. Workshop, Hangzhou, China, 2020.

[30] H. Godrich, A. P. Petropulu, H. V. Poor, Sensor selection in distributed multiple-radar architectures for localization: A knapsack problem formulation, IEEE Trans. Signal Process. 60 (1) (2012) 247–260. `doi:10.1109/TSP.2011.2170170`.

[31] O. Mehanna, N. D. Sidiropoulos, G. B. Giannakis, Joint multicast beamforming and antenna selection, IEEE Trans. Signal Process. 61 (10) (2013) 2660–2674. `doi:10.1109/TSP.2013.2252167`.

[32] O. T. Demir, T. E. Tuncer, Antenna selection and hybrid beamforming for simultaneous wireless information and power transfer in multi-group multicasting systems, IEEE Trans. Wireless Commun. 15 (10) (2016) 6948–6962. `doi:10.1109/TWC.2016.2594074`.

[33] L. Blanco, M. Njar, Sparse multiple relay selection for network beamforming with individual power constraints using semidefinite relaxation, IEEE Trans. Wireless Commun. 15 (2) (2016) 1206–1217. `doi:10.1109/TWC.2015.2487439`.

[34] H. Nosrati, E. Aboutanios, D. Smith, Array partitioning for multi-task operation in dual function MIMO systems, Digital Signal Process. 82 (2018) 106 – 117. `doi:https://doi.org/10.1016/j.dsp.2018.06.019`.

34

URL   `http://www.sciencedirect.com/science/article/pii/`
`S1051200418305499`

[35] A. Deligiannis, M. Amin, S. Lambotharan, G. Fabrizio, Optimum sparse subarray design for multitask receivers, IEEE Trans. Aerosp. Electron. Syst. 55 (2) (2019) 939–950. `doi:10.1109/TAES.2018.2867258`.

[36] X. Wang, A. Hassanien, M. G. Amin, Sparse transmit array design for dual-function radar communications by antenna selection, Digital Signal Process. 83 (2018) 223–234.

[37] X. Wang, A. Hassanien, M. G. Amin, Dual-function MIMO radar communications system design via sparse array optimization, IEEE Trans. Aerosp. Electron. Syst. 55 (3) (2019) 1213–1226. `doi:10.1109/TAES.2018.`
`2866038`.

[38] A. Koochakzadeh, P. Pal, Beam-pattern design for hybrid beamforming using wirtinger flow, in: Proc. IEEE Int. Workshop Signal Process. Advances in Wireless Commun., Kalamata, Greece, 2018.

[39] E. J. Candès, M. B. Wakin, S. P. Boyd, Enhancing sparsity by reweighted l_1 minimization, Journal of Fourier Analysis and Applications 14 (5) (2008) 877–905. `doi:10.1007/s00041-008-9045-x`.

[40] K. Lange, Optimization, Springer, New York, 2004.

[41] M. Yuan, Y. Lin, Model selection and estimation in regression with grouped variables, J. R. Stat. Soc. B. 68 (2006) 49–67. `doi:10.1111/j.1467-9868.`
`2005.00532.x`.

[42] F. Bach, R. Jenatton, J. Mairal, G. Obozinski, Optimization with sparsity-inducing penalties, Found. Trends Mach. Learn. 4 (1) (2012) 1–106. `doi:`
`10.1561/2200000015`.

[43] K. C. Toh, M. J. Todd, R. H. Ttnc, SDPT3 - A Matlab software package for semidefinite programming, version 1.3, Optim. Methods. Softw. 11 (1-4) (1999) 545–581. `doi:10.1080/10556789908805762`.

[44] CVX Research, Inc., CVX: Matlab software for disciplined convex pro-
gramming, version 2.0, `http://cvxr.com/cvx` (Aug. 2012).

630